Separation Science and Technology
Publication details, including instructions for authors and subscription information:
http://www.informaworld.com/smpp/title~content=t713708471

Groundwater Cleanup by *in-situ* Sparging. V. Mass Transport-Limited Dense Nonaqueous Phase Liquid and Volatile Organic Compound Removal

David J. Wilson[a]
[a] DEPARTMENT OF CHEMISTRY, VANDERBILT UNIVERSITY, NASHVILLE, TENNESSEE

To cite this Article Wilson, David J.(1994) 'Groundwater Cleanup by *in-situ* Sparging. V. Mass Transport-Limited Dense Nonaqueous Phase Liquid and Volatile Organic Compound Removal', Separation Science and Technology, 29: 1, 71 — 91
To link to this Article: DOI: 10.1080/01496399408002470
URL: http://dx.doi.org/10.1080/01496399408002470

SEPARATION SCIENCE AND TECHNOLOGY, **29**(1), pp. 71–91, 1994

Groundwater Cleanup by *in-situ* Sparging. V. Mass Transport-Limited Dense Nonaqueous Phase Liquid and Volatile Organic Compound Removal

DAVID J. WILSON
DEPARTMENT OF CHEMISTRY
VANDERBILT UNIVERSITY
NASHVILLE, TENNESSEE 37235

ABSTRACT

A mathematical model is presented for the removal of dense nonaqueous phase liquid (DNAPL) droplets in an aquifer by air sparging with a horizontal slotted pipe. Diffusion transport of volatile organic compounds (VOCs) from the DNAPL droplets to the aqueous phase is assumed to take place through a thick stagnant water layer in the porous medium to a mobile aqueous phase. Transport of VOC from the aqueous phase into the gas phase is modeled by means of a lumped parameter approach. The air-induced circulation of water in the vicinity of the air injection pipe is modeled by means of the method of images. The effects of the various model parameters on the rate of VOC removal are explored both for cases in which DNAPL is present and in which contaminant is present only as VOC dissolved in the aqueous phase.

INTRODUCTION

There is presently considerable interest in the use of air sparging for the removal of such dense nonaqueous phase liquids (DNAPLs) as trichloroethylene, 1,1,1-trichloroethane, tetrachloroethylene, and the dichloroethylenes from aquifers contaminated with compounds of this type. Schwille's (1) experimental work visualized for us how these compounds move rapidly down through an aquifer, leaving a trail of residual DNAPL blobs trapped interstitially in the aquifer medium. Feenstra and Cherry (2) reviewed the subject of DNAPLs in groundwater, and Powers et al. (3, 4) investigated the kinetics of solution of these blobs of DNAPL. There

appears to be general agreement that the low rates of removal of DNAPL achieved by such technologies as pump-and-treat are associated with severely limited rates of mass transport between the nonaqueous and aqueous phases and with the tendency of the mobile aqueous phase to bypass contaminated regions of low permeability. There is some hope that air sparging techniques may provide more rapid remediation of such sites.

Herrling and Stamm (5) discussed a modification of this technique, vacuum-vaporizer-wells, which is in use in Germany, and Brown (6, 7) described sparging by means of simple air injection wells. We developed models for sparging dissolved VOCs by use of an aeration curtain at right angles to the groundwater flow (8) and by means of a simple air injection well (9). More recently we addressed the modeling of DNAPL removal by means of the vacuum-vaporizer-well configuration and by aeration curtains (10), as well as by means of a sparging well configured either as a single vertical pipe screened at the bottom (cylindrical coordinates) or as a horizontal slotted pipe (Cartesian coordinates) (11).

In our work on modeling the sparging of DNAPLs we assumed that the kinetics of solution of the DNAPL blobs could be a severely rate-limiting step, but that the rate of mass transport of VOC from the aqueous phase to the moving gas stream could be adequately described by a local equilibrium approximation. In the modeling of the operation of simple sparging wells it was further assumed that the movement of air through the aquifer did not bring about significant circulation of water. In the present work we eliminate both of those approximations. The kinetics of mass transfer between the aqueous phase and the vapor phase is handled by means of a lumped parameter method which we have used previously (12). The air-induced circulation of water is represented by introducing the flow field resulting from a source at the top of the aquifer and a corresponding sink at the bottom; discharge to the sink is shunted to the source so that the flow field is conservative. Here we deal with sparging by means of a horizontal slotted pipe of length long compared to its breadth of influence, which permits the use of a two-coordinate Cartesian system if end effects are ignored.

ANALYSIS

Modeling the Volumetric Gas Flow Field

Parameters in the model are defined as follows:

l = length of horizontal slotted pipe, m
h = thickness of aquifer, m
Q_a = molar gas flow rate, mol/s

We assume a molar gas flux in the z-direction (vertical) of

$$q_z(x, y) = A[a_0^2(z/h) - x^2] \tag{1}$$

where A = a function of z to be determined by conservation requirements
a_0 = effective half-width of gas distribution at the top of the aquifer, m

As shown in Ref. 11, this leads to the following expressions for the components of the molar gas flux:

$$q_x(x, z) = \frac{3Q_a h^{3/2}}{8a_0^3 l} \frac{x}{z^{5/2}} [a_0^2(z/h) - x^2] \tag{2}$$

$$q_z(x, z) = \frac{3Q_a h^{3/2}}{4a_0^3 l} \frac{1}{z^{3/2}} [a_0^2(z/h) - x^2] \tag{3}$$

if $x^2 < a_0^2(z/h)$, q_x and $q_z = 0$ if $x^2 > a_0^2(z/h)$.

The volumetric gas flux components are then given by

$$S_x = (RT/P)q_x \tag{4}$$

$$S_z = (RT/P)q_z \tag{5}$$

where R = gas constant, $m^3 \cdot atm/mol \cdot deg$
T = temperature, °K
P = local pressure, atm

We assume that the local pressure is adequately approximated by the sum of the ambient atmospheric pressure and the hydrostatic pressure, which gives

$$P = P(z) = P_a + \sigma(h - z) \tag{6}$$

where P_a = ambient pressure (typically 1 atm)
= 1 atm/10.336 m

Modeling the Air-Flow-Induced Water Flow Field

We assume that the water circulation induced by the injected air can be described adequately by the flow field generated by a water source Q_w at the top of the aquifer (at $x = 0$, $z = h$), and a water sink $-Q_w$ at the bottom of the aquifer (at $x = 0, z = 0$). We assume no-normal-flow boundary conditions at the top and bottom of the aquifer. Then, as detailed in Ref. 9, one can easily generate the velocity potential by the method of images from electrostatics. This, in turn, yields the following expressions for the water fluxes v_x and v_z.

$$v_x = \frac{Q_w}{\pi l} \sum_{n=-\infty} \left[\frac{x}{x^2 + [z - (2n + l)h]^2} - \frac{x}{x^2 + [z - 2nh]^2} \right] \quad (7)$$

$$v_y = \frac{Q_w}{\pi l} \sum_{n=-\infty} \left[\frac{z - (2n + l)h}{x^2 + [z - (2n + l)h]^2} - \frac{z - 2nh}{x^2 + [z - 2nh]^2} \right] \quad (8)$$

Here Q_w, the magnitude of the source and the sink generating the water flow field, is a function of the aquifer thickness h, the permeability of the aquifer medium, and Q_a, the air flow rate through the sparging well. Presumably Q_w will have to be determined on a site-specific basis

Solution of DNAPL Droplets: Equations for the C_{ij}

We use a method for representing the solution of DNAPL droplets which was employed in our earlier DNAPL sparging models (10, 11) and which was originally developed for use in modeling pump-and-treat operations in aquifers contaminated with DNAPL (13). The physical picture for the process is that of a spherical DNAPL droplet from which VOC is dissolving and diffusing through a thick stagnant water layer in the porous medium to the moving aqueous phase (which is in contact with the vapor phase). Analysis of this picture of the DNAPL solution process then gives (12)

$$\frac{dC_{ij}}{dt} = - \frac{3C_0^{2/3} D(c_s - c_{ij}^w) C_{ij}^{1/3}}{\rho a_0^2} \quad (9)$$

where C_{ij} = concentration of DNAPL in the ijth volume element of the system, kg/m^3

C_0 = initial concentration of DNAPL in the contaminated portion of the system, kg/m^3

c_{ij}^w = aqueous concentration of VOC in the ijth volume element, kg/m^3 of aqueous phase

c_s = saturation concentration of VOC in water, kg/m^3

D = diffusivity of VOC in the water-saturated porous medium, m^2/s

ρ = DNAPL density, kg/m^3

a_0 = initial DNAPL droplet radius, m

Material Balance for the Aqueous Phase: Equations for the c_{ij}^w

On carrying out a material balance on the VOC in the aqueous phase in the ijth volume element, we obtain the following set of equations.

$$\omega \Delta x \Delta z l \frac{dc_{ij}^w}{dt} = -\Delta x \Delta z l \frac{dC_{ij}}{dt} - \Delta x \Delta z l (\nu - \omega)\lambda (K_H c_{ij}^w - c_{ij}^g)$$

$$+ \Delta z l v_x \left[(i-1)\Delta x, \left(j - \frac{1}{2}\right)\Delta z \right] T(v_x) c_{i-1,j}^w$$

$$- \Delta z l v_x \left[i\Delta x, \left(j - \frac{1}{2}\right)\Delta z \right] T(-v_x) c_{i+1,j}^w$$

$$+ \Delta x l v_z \left[\left(i - \frac{1}{2}\right)\Delta x, (j-1)\Delta z \right] T(v_z) c_{i,j-1}^w$$

$$- \Delta x l v_z \left[\left(i - \frac{1}{2}\right)\Delta x, j\Delta z \right] T(v_z) c_{i,j+1}^w \qquad (10)$$

$$+ \left\{ \Delta z l v_x \left[(i-1)\Delta x, \left(j - \frac{1}{2}\right)\Delta z \right] T(-v_x) \right.$$

$$- \Delta z l v_x \left[i\Delta x, \left(j - \frac{1}{2}\right)\Delta z \right] T(v_x)$$

$$+ \Delta x l v_z \left[\left(i - \frac{1}{2}\right)\Delta x, (j-1)\Delta z \right] T(-v_z)$$

$$\left. - \Delta x l v_z \left[\left(i - \frac{1}{2}\right)\Delta x, j\Delta z \right] T(v_z) \right\} c_{ij}^w$$

In Eq. (10) the first term on the right-hand side represents mass transport of VOC into the aqueous phase from DNAPL droplets. The second term represents a lumped parameter approximation for mass transport of VOC between the aqueous phase and the vapor phase. The remaining eight terms represent advective transport of aqueous VOC between the volume element of interest and its nearest neighbors. Here

ν = total porosity of the aquifer medium
ω = water-filled porosity of the medium
K_H = Henry's constant for the VOC, dimensionless
λ = lumped parameter rate constant for mass transport of VOC between the aqueous and vapor phases, s^{-1}
c_{ij}^g = vapor phase VOC concentration in the ijth volume element, kg/m^3

The function $T(v)$ is a switching function equal to zero if its argument is negative and equal to one if its argument is positive. In Eq. (10) the arguments of T in the various terms are the velocities which precede T in each term.

To close the loop on the water circulation field and prevent unphysical accumulation of contaminant in the 1,1-th volume element, we introduce a shunt along the axis of the system (i.e., along the left side of the half of the system being modeled) to transport the water entering the 1,1-th volume element at the bottom of the aquifer back up to the $1,n_z$-th volume element at the top. This requires modifying Eqs. (10) by subtracting a term $(Q_w/4)c_{11}^w$ from the 1,1-th equation and adding an identical term to the $1,n_z$-th equation. The 4 in the denominator is required by the fact that the 1,1-th and $1,n_z$-th volume elements handle only one-fourth of the total flow used to generate the water flow field, since the sink and the source are located on the lower left and upper left edges of these volume elements, respectively.

Material Balance for the Vapor Phase: The Steady-State Approximation for the c_{ij}^g

Construction of a mass balance for vapor phase VOC in the ijth volume element yields

$$
\begin{aligned}
(v-\omega)l\Delta x\Delta z\frac{dc_{ij}^g}{dt} = {} & (v-\omega)l\Delta x\Delta z\lambda(K_{\mathrm{H}}c_{ij}^w - c_{ij}^g) \\
& + l\Delta x S_z\left[\left(i-\frac{1}{2}\right)\Delta x,\ (j-1)\Delta z\right]\frac{P\left[\left(j-\frac{3}{2}\right)\Delta z\right]}{P[(j-1)\Delta z]} \\
& \times c_{i,j-1}^g + l\Delta z S_x\left[(i-1)\Delta x,\ \left(j-\frac{1}{2}\right)\Delta z\right]c_{i-1,j}^g \qquad (11) \\
& - l\Delta x S_z\left[\left(i-\frac{1}{2}\right)\Delta x,\ j\Delta z\right]\frac{P[j\Delta z]}{P\left[\left(j-\frac{1}{2}\right)\Delta z\right]} \\
& \times c_{ij}^g - l\Delta z S_x\left[i\Delta x,\ \left(j-\frac{1}{2}\right)\Delta z\right]c_{ij}^g
\end{aligned}
$$

The first term on the right-hand side of Eq. (11) corresponds to mass transport of VOC between the vapor and aqueous phases. The next four

terms correspond to advective transport of VOC vapor by the sparging gas. It is necessary to include pressure ratio factors in two of these terms to take into account the dilution of VOC in the vapor as it rises into regions of lower pressure; if this is not done, the advective terms do not conserve VOC. The form of the volumetric gas flux here makes it unnecessary to include in these equations the switching terms needed in describing advection in the aqueous phase.

The system of Eqs. (9), (10), and (11) which has been developed to model DNAPL sparging is a mathematically stiff set of differential equations. That is, although one can expect experimental runs in the field to require some months, the time increments which one must use in the numerical integration of the model equations must be of the order of 10 seconds or less. This leads to excessive computer time requirements. One can get around this difficulty by noting the fact that generally the mass of VOC in the vapor phase is only a very small fraction of the total mass of VOC present in the system. This suggests that one may be able to use the steady-state approximation for the vapor-phase concentrations. In this, one sets the left-hand side of Eq. (11) equal to zero and then solves the resulting algebraic equation for c_{ij}^g, starting with the equation for c_{11}^g and going in the directions of increasing i and j. This process converts the stiff differential equations into algebraic equations, and thereby permits the use of very much larger values of the time increment Δt in the numerical integrations. A comparison of results of the exact approach and the steady-state approach for a representative set of parameters is given in Table 1; we see that the discrepancy is less than 0.1%. In all of the work presented here, the steady-state approximation was used.

One of the points of interest is the extent to which the form of the molar gas flux $q_z(x, z)$ influences the modeling results. This function was chosen somewhat arbitrarily to be given by Eq. (1), so it would be helpful if one could show that the calculated cleanup rates were not highly sensitive to the form of Eq. 1). We next explore this point.

Let us replace Eq. (1) for $q_z(x, z)$ by Eq. (12):

$$\begin{aligned} q_z(x, z) &= A(z)[a_0^n z/h - x^n], \qquad |x| < a_0(z/h)^{1/n} \\ &= 0, \qquad |x| > a_0(z/h)^{1/n} \end{aligned} \tag{12}$$

Note that Eq. (1) simply corresponds to the case $n = 2$. One follows along the lines of the development of Ref. 11. The requirement that the integral of $q_z(x, z)$ over any plane perpendicular to the z-axis gives Q_a, the total molar gas flow rate, yields

$$A(z) = \frac{Q_a(n+1)}{2nla_0^{n+1}} (h/z)^{(n+1)/n} \tag{13}$$

TABLE 1
Comparison of the Results of Steady-State and Nonsteady-State Model Calculations[a,b]

Time (days)	Total remaining VOC (kg)	
	Steady-state	Nonsteady-state
0	1902.40	1902.40
1	1759.39	1759.51
2	1657.21	1657.32
3	1558.67	1558.79
4	1462.09	1462.19
5	1367.49	1367.59
6	1275.07	1275.18
7	1185.04	1185.14
8	1097.65	1097.74
9	1013.22	1013.31
10	932.15	932.25
11	854.98	855.09
12	782.44	782.55
13	715.60	715.71
14	656.23	656.35

[a] The parameters used in these calculations are those given in Table 2 except that $Q_a = 1.0$ mol/s and $Q_w = 0$.
[b] In the steady-state runs, $dt = 100$ seconds. In the nonsteady-state runs, $dt = 10$ seconds.

The molar gas flux is conservative, so its divergence must vanish. This yields

$$\frac{\partial q_z}{\partial z} = -\frac{\partial q_x}{\partial x} \tag{14}$$

Differentiating the expression for q_z with respect to z and then integrating with respect to x yields an expression for $q_x(x, z)$. Note that the integration constant is easily evaluated from the fact that the symmetry of the problem gives $q_x(0, z) = 0$. The final results for q_z and q_x are

$$q_z = \frac{Q_a(n+1)}{2nla_0}(h/z)^{1/n}[1 - (h/z)(x/a_0)^n] \tag{15}$$

and

$$q_x = \frac{Q_a(n+1)}{2n^2lh}(x/a_0)(h/z)^{(n+1)/n}[1 - (h/z)(x/a_0)^n] \tag{16}$$

The remainder of the analysis follows exactly along the lines described above.

RESULTS

The model was implemented in TurboBASIC, and the runs described below were made on microcomputers equipped with 80286 or 80386 microprocessors operating at 12 and 33 mHz, respectively, and equipped with math coprocessors. Typical runs required a half hour or less of computer time.

Default parameters used in the modeling are given in Table 2. Where other values of parameters were used, these are indicated in the legends of the figures.

The effect of the parameter controlling mass transport of VOC between the aqueous and vapor phases, λ, on rate of VOC removal is shown in Fig. 1. For the parameter sets being used it is evident that this mass transport step is quite significant in controlling the rate of removal. Evidently one would be well-advised to explore methods to increase the

TABLE 2
Default Sparging Model Parameters, DNAPL Runs

Width of domain of interest	10 m
Thickness of aquifer	5 m
Length of horizontal sparging pipe	20 m
n_x, n_z	5, 5
Width of air sparging pattern at top of aquifer	10 m
Molar gas flow rate of sparging well	4 mol/s
Air-induced water circulation rate	4 L/s
Ambient temperature	20°C
Total porosity of aquifer medium	0.4
Water-filled porosity of aquifer medium	0.36
Aquifer medium density	1.7 mg/cm^3
Contaminant	Trichloroethylene
Density of contaminant	1.46 g/cm^3
Water solubility of contaminant	1100 mg/L
Henry's constant of contaminant (dimensionless)	0.20
Diffusivity of contaminant in porous medium	2×10^{-10} m^2/s
Rate constant λ for aqueous phase/vapor transport	0.001 s^{-1}
Initial DNAPL concentration	2000 mg/kg
Initial dissolved VOC concentration	1100 mg/L water
Width of contaminated zone	8 m
Depth of contaminated zone below water table	3 m
Initial DNAPL droplet diameter	0.1 cm
dt	100 seconds

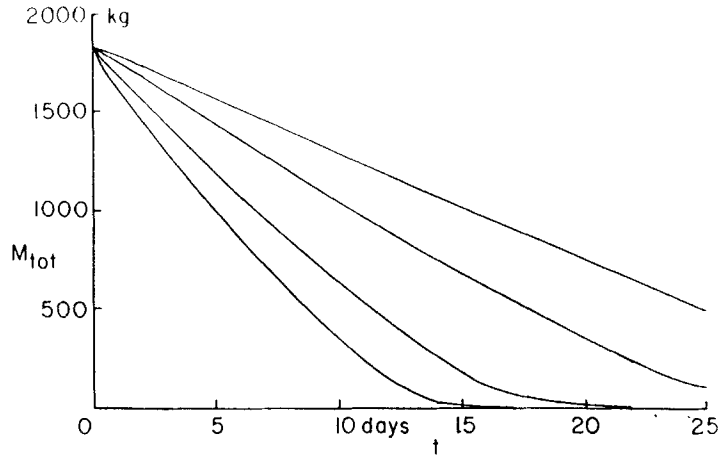

FIG. 1 Plots of residual mass of TCE versus time; effect of aqueous phase-vapor transport parameter λ. From top to bottom, λ = 1, 2, 5, and 10 × 10^{-4} $second^{-1}$. Other parameters as in Table 2.

amount of air–water interface present during sparging operations, since this should result in increased values of λ.

The impact of air flow rate Q_a on VOC removal rate is seen in Fig. 2. It is apparent that, over the range of air flow rates used, air flow rate is not appreciably limiting. For example, doubling the air flow rate from 1 to 2 mol/s results in a barely detectable increase in VOC removal rate. In an actual sparging operation, one would probably want to work at the lower end of the air flow rate range to avoid the costs of pumping excessive amounts of air and of treating excessive volumes of highly dilute off-gas if this is being recovered for treatment.

The effect of water circulation rate Q_w on the VOC removal rate is relatively slight, as seen in Fig. 3. In practice, one is not able to vary this parameter independently as it is presumably determined by the air flow rate, the well design, and the geological characteristics of the site. For the runs made here, a zero value of Q_w resulted in an unremovable residue of VOC which was outside the zone of influence of the air. In field operations this parameter would probably be quite difficult to measure, so perhaps one is fortunate that the role it plays is minor.

The parameter controlling the width of influence of the air injection well, a_0, is certainly linked to the geological characteristics of the aquifer, to the well design, and to the rate at which air is being injected. Figure 4 shows that it is undesirable to have values of the width parameter which

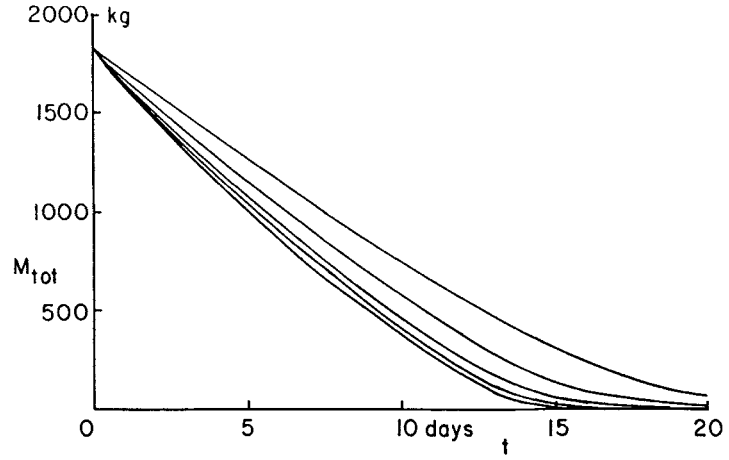

FIG. 2 Plots of residual mass of TCE versus time; effect of air injection rate Q_a. From top to bottom, Q_a = 0.125, 0.25, 0.5, 1, and 2 mol/s. Other parameters as in Table 2.

are sufficiently small that portions of the zone of contamination are not aerated. Removal rates are decreased, and we may have a significant increase in tailing if the VOC must be dissolved and then circulated to the aeration zone in order to be removed. Sparging pilot studies should result in site-specific information on the relationship between the width

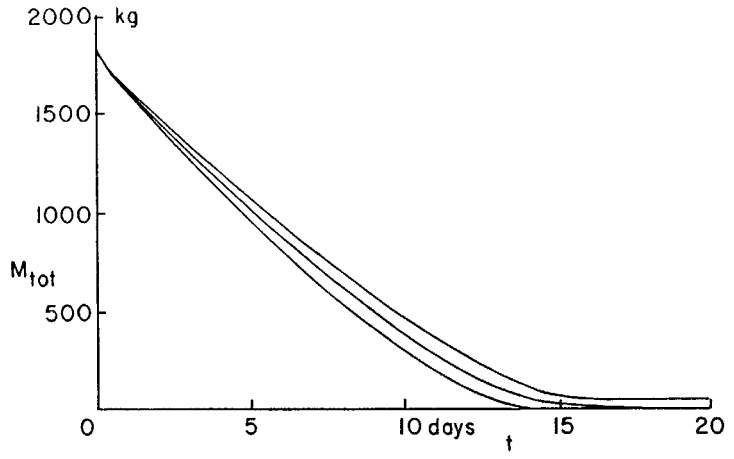

FIG. 3 Plots of residual mass of TCE versus time; effect of water circulation rate Q_w. From top to bottom, Q_w = 0, 2, and 10 L/s. Other parameters as in Table 2.

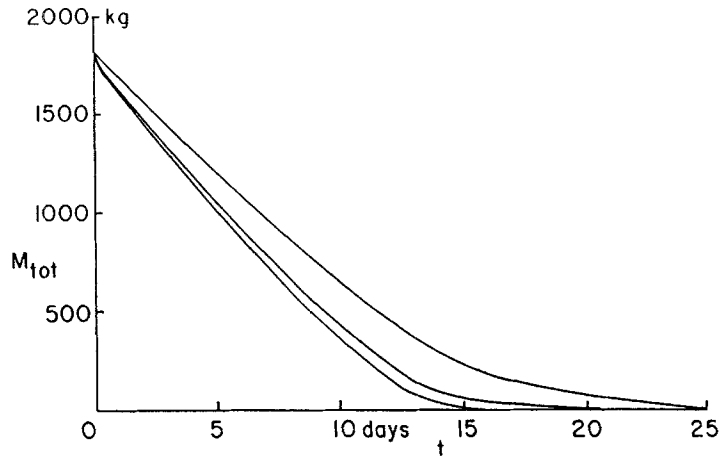

FIG. 4 Plots of residual mass of TCE versus time; effect of air distribution width parameter a_0. a_0 = 6, 8, and 10 m, top to bottom. Other parameters as in Table 2.

parameter and the air injection rate. This presumably can be obtained by placing piezometer wells close to the water table at various distances from the air injection well and monitoring soil gas pressure as a function of air injection rate and distance from the injection well.

The effect of effective DNAPL droplet diameter on removal rate is shown in Fig. 5. Increasing the effective DNAPL droplet diameter decreases the surface to volume ratio of the DNAPL in the aquifer, thereby decreasing the rate of solution of DNAPL. Initially these runs all show a rather rapid rate of cleanup, during which dissolved VOC is being removed. Once this has been done, however, the rate of solution of the DNAPL droplets/ganglia/blobs becomes a major factor in controlling the rate of the remediation. Pilot studies must be carried out for a period sufficient to give an indication of the extent to which this type of mass transport will be rate-limiting if they are to be useful in estimating remediation times.

The dependence of removal rate on the form of the air flux function $q_z(x, y)$ is shown in Fig. 6. In the results shown in this figure the molar gas fluxes were calculated using Eqs. (15) and (16) with n = 0.5, 1, 2, 3, 4, and 10. It is easily seen from Eq. (15) that the larger values of n give a flux of sparging gas which is more uniformly distributed across the domain of interest than do the smaller values of n. This is reflected in the somewhat more rapid removal rates observed for the runs having the larger values of n. It is of interest to note, however, that varying n from

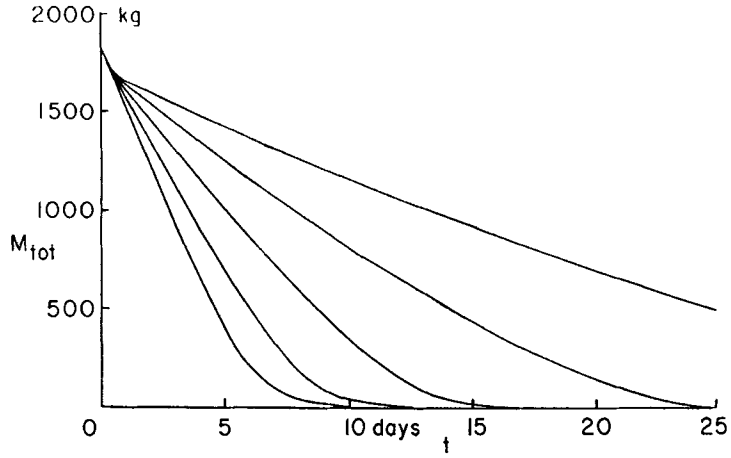

FIG. 5 Plots of residual mass of TCE versus time; effect of effective DNAPL droplet diameter. Droplet diameter = 0.2, 0.1414, 0.1, 0.0707, and 0.05 cm, top to bottom. Other parameters as in Table 2.

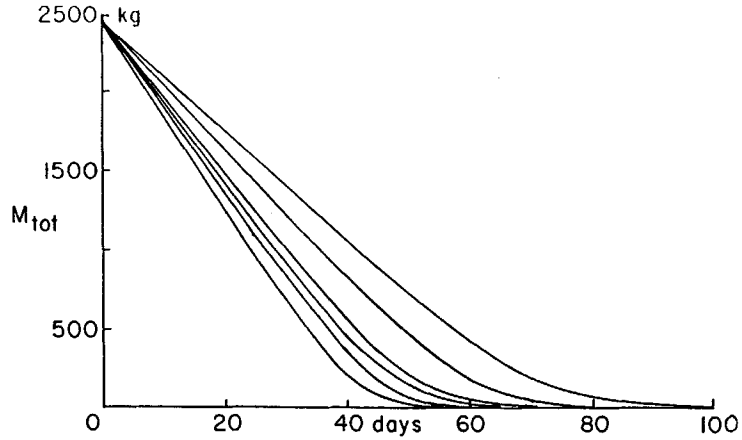

FIG. 6 Plots of residual mass of TCE versus time; effect of the parameter n in the sparging gas molar flux function $q_z(x, z)$. n = 0.5, 1, 2, 3, 4, and 10 from top to bottom; gas flow rate of sparging well = 2 mol/s; rate constant for aqueous phase/vapor phase mass transport = 0.0001 second^{-1}. Other parameters as in Table 2.

10 all the way to 1 results in only about a 30% increase in the time required for cleanup. With some relief we therefore conclude that cleanup times are not very sensitive to the precise form of the distribution of the sparging gas. This is quite fortunate, since this distribution would be quite difficult to calculate and also quite difficult to measure experimentally.

In earlier work (9) we modeled the removal of dissolved VOC by sparging using an approach in which the domain of influence of the sparging well was partitioned into two one-dimensional (radial) sets of annular cylindrical domains for computation. One set modeled the upper half of the aquifer, the second the lower half. For sparging with a horizontal slotted pipe, the computer program used in the present calculations allows us to eliminate this simplification. In Figs. 7 through 11 we present the results of runs simulating the removal of dissolved VOC (in the absence of DNAPL) by sparging with a horizontal slotted pipe. In these calculations the initial DNAPL concentrations were set equal to zero, and the initial dissolved VOC concentrations were set equal to a value below the aqueous solubility of the VOC. Default parameters for these runs are given in Table 3.

TABLE 3
Default Sparging Model Parameters, Dissolved VOC Runs

Width of domain of interest	10 m
Thickness of aquifer	5 m
Length of horizontal sparging pipe	20 m
n_x, n_z	5, 5
Width of air sparging pattern at top of aquifer	10 m
Molar gas flow rate of sparging well	1 mol/s
Air-induced water circulation rate	1 L/s
Ambient temperature	20°C
Total porosity of aquifer medium	0.4
Water-filled porosity of aquifer medium	0.36
Aquifer medium density	1.7 mg/cm^3
Contaminant	Trichloroethylene
Density of contaminant	1.46 g/cm^3
Water solubility of contaminant	1100 mg/L
Henry's constant of contaminant (dimensionless)	0.20
Diffusivity of contaminant in porous medium	2×10^{-10} m^2/s
Rate constant λ for aqueous phase/vapor transport	0.001 s^{-1}
Initial DNAPL concentration	0 mg/kg
Initial dissolved VOC concentration	1000 mg/L water
Width of contaminated zone	8 m
Depth of contaminated zone below water table	3 m
Initial DNAPL droplet diameter	0.1 cm
dt	100 seconds

In Fig. 7 we see the effect of the mass transfer rate parameter λ for transport of VOC from the aqueous phase to the vapor phase. As expected, the rate of cleanup can be extremely adversely affected if λ is small. The value of λ should increase with increasing air–water interfacial area within the aquifer and with increasing uniformity of distribution of the injected gas flux. These are parameters which would be extremely difficult (if not impossible) to measure or estimate by laboratory experiments, and they may also be rather site-specific. One must therefore plan on experimental estimation of λ during the course of pilot-scale experiments at the site. This, in turn, dictates that the pilot-scale sparging runs be of sufficient duration to allow one to get a reasonably accurate estimate of λ. We note that initial VOC removal rates (from water lying in the near vicinity of air channels) may be much more rapid than the rate which will be sustained after the easily removable VOC has been sparged out and one is removing VOC which may have to move by aqueous advection or by diffusion into a region from which it may readily be air stripped.

In Fig. 8 the effect of Henry's constant is shown. Henry's constants are known for all of the environmentally significant VOCs [see Montgomery and Welkom (14), for example], so the effects of this parameter are readily predicted unless the aquifer medium contains substantial quantities of clay or other material which may sorb the contaminants. If such materials are present, one may expect this to result in the determination of small values of λ during pilot studies, since these will not distinguish

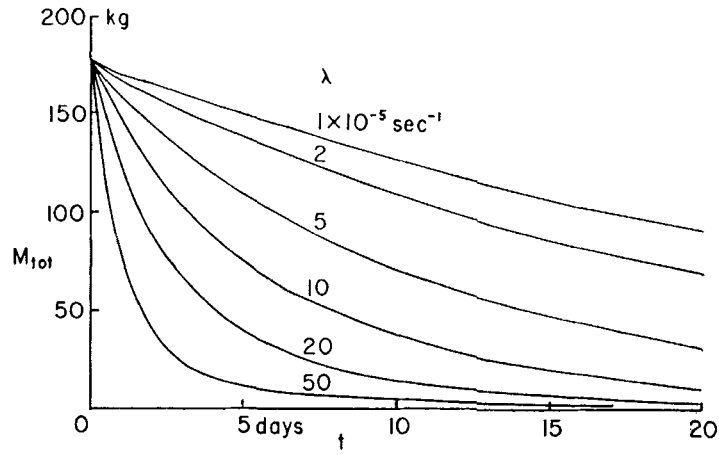

FIG. 7 Plots of total residual VOC mass versus time (no DNAPL present); effect of aqueous/vapor mass transfer rate parameter λ. Default parameters are given in Table 3.

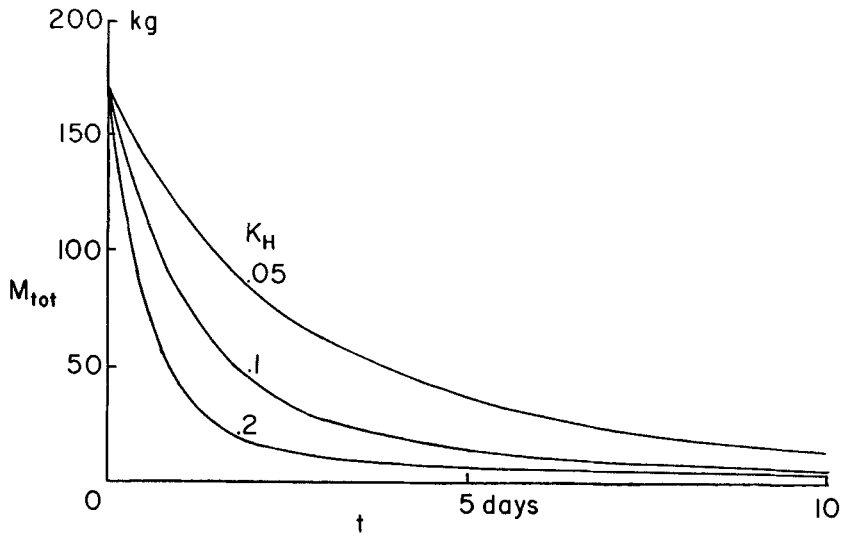

FIG. 8 Plots of total residual VOC mass versus time (no DNAPL present); effect of Henry's constant K_H. Default parameters are given in Table 3.

between slow aqueous-vapor mass transport kinetics and slow desorption or diffusion kinetics.

The effects of the width parameter of the air distribution, a_0, are shown in Fig. 9. The effects are not large until the width parameter is sufficiently small that portions of the zone of contamination lie outside the domain through which air is passing. When that occurs, as is the case with the curve for which $a_0 = 6$ m, the dissolved VOC must move by relatively slow advection into the domain through which the air is passing before it can be removed by stripping. This results in relatively severe tailing; evidently for expeditious cleanup, one should design sparging systems in such a fashion that air is delivered to all of the volume of the aquifer which is contaminated.

Figure 10 shows that the effect of the rate of air-induced water circulation (Q_w) on the rate of dissolved VOC removal is relatively slight for the system modeled. A relatively slight effect was also found to be the case when DNAPL was being removed; see Fig. 3. In the Fig. 10 runs, as well as those shown in Fig. 3, the zone of contamination lies entirely within the domain which is being aerated. One expects that the effect of Q_w on VOC removal rate would be somewhat larger if there were portions of the zone of contamination which were outside of the domain of aeration; this point was explored and found out to be in fact the case. The order

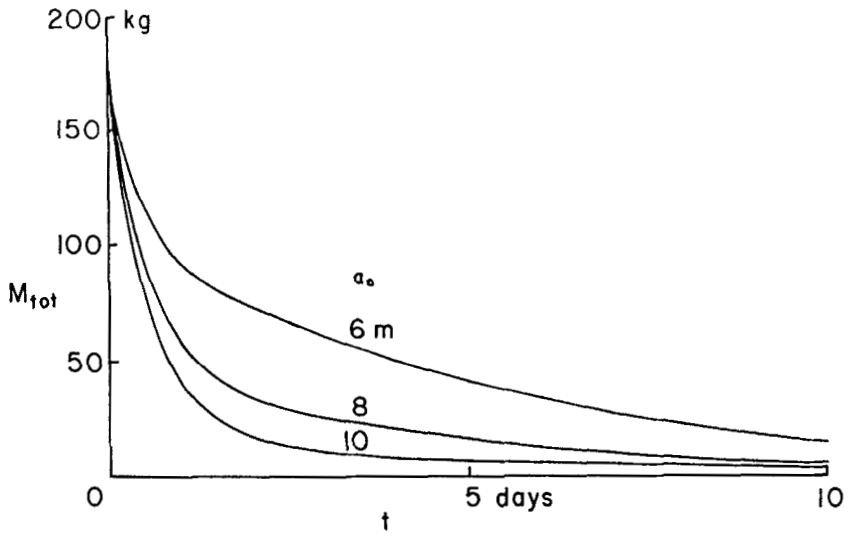

FIG. 9 Plots of total residual VOC mass versus time (no DNAPL present); effect of the width parameter a_0 of the air distribution. Default parameters as in Table 3.

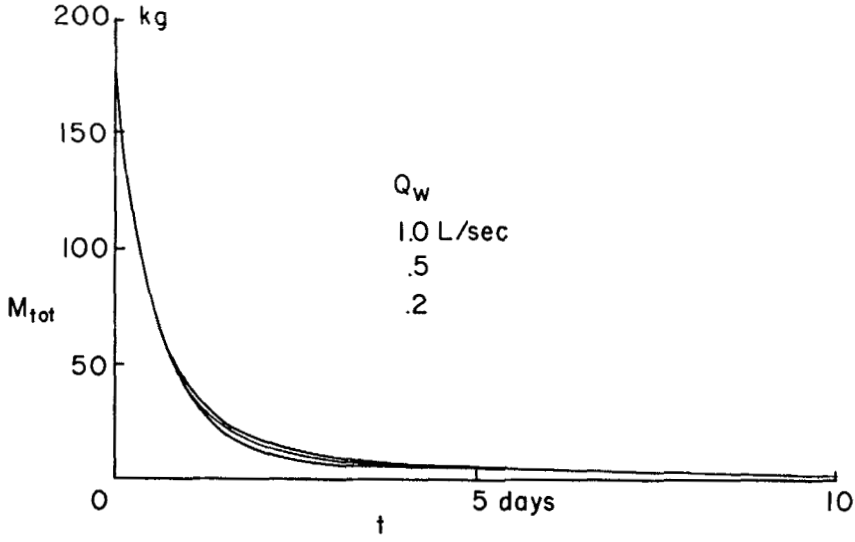

FIG. 10 Plots of total residual VOC mass versus time (no DNAPL present); effect of the air-induced water circulation rate Q_w. Default parameters as in Table 3.

of the curves appears at first to be counterintuitive, in that increasing Q_w actually causes a slight *decrease* in the rate of VOC removal. Examination of the actual distribution of VOC in the simulated aquifer in greater detail revealed that an increased water circulation rate carried VOC more rapidly out of the domain through which air was moving than was the case at a lower water circulation rate. Once this VOC has left the region in which sparging is actually occurring, it cannot be removed until it is carried back into that domain. Eventually, of course, this does occur, which is why the three curves merge after about 4 days' sparging.

The impact of sparging air flow rate Q_a on the VOC removal rate is shown in Fig. 11. The results, however, require some interpretation. If the removal is strictly limited by the ability of the air to carry VOC (i.e., when there is local equilibrium between the vapor and the aqueous phase with respect to VOC transport), the removal rate is directly proportional to the air flow rate. If the air flow rate is large, so that removal is strictly limited by the rate of mass transport between the aqueous and vapor phases, one expects the removal rate to be proportional to the air–water interfacial area, so that the removal rate would again be proportional to the air flow rate. This dependence would be handled in our model by means of a proportional increase in the value of λ, the aqueous-vapor

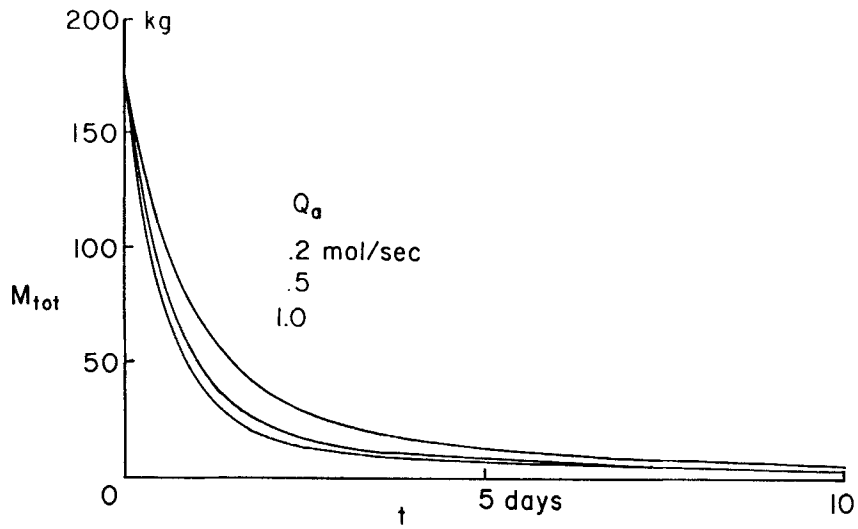

FIG. 11 Plots of total residual VOC mass versus time (no DNAPL present); effect of the sparging air molar flow rate Q_a. In these runs the aqueous-vapor VOC mass transfer rate parameter λ is held constant at 0.001 second^{-1}. Default parameters as in Table 3.

VOC mass transfer rate parameter. In Fig. 11, however, the value of λ was held constant, and only Q_a was varied. We therefore observe a substantially weaker dependence of removal rate on Q_a than direct proportionality.

Figure 12 shows a set of plots in which Q_a is again varied (as in Fig. 11); however, the values of λ were chosen to be proportional to the values of Q_a. We see, as anticipated, a much stronger dependence of removal rate on Q_a in Fig. 12 than was observed in Fig. 11. In fact, these curves are superimposed if they are plotted on a reduced time scale of $Q_a t/(1$ mol/s).

The plots in Fig. 13 show the effects of variations in Q_a, with proportional variations in Q_w and λ. Earlier, in Figs. 1, 2, and 3, these parameters were varied singly. Physically, one would expect both Q_w and λ to increase with increasing Q_a, although the precise nature of the dependence is uncertain. Removal rates do increase with increasing Q_w, Q_a, and λ, as was seen in Fig. 12 for the sparging of dissolved VOC. However, as the air flow rate becomes larger, the rate of mass transfer from the droplets to

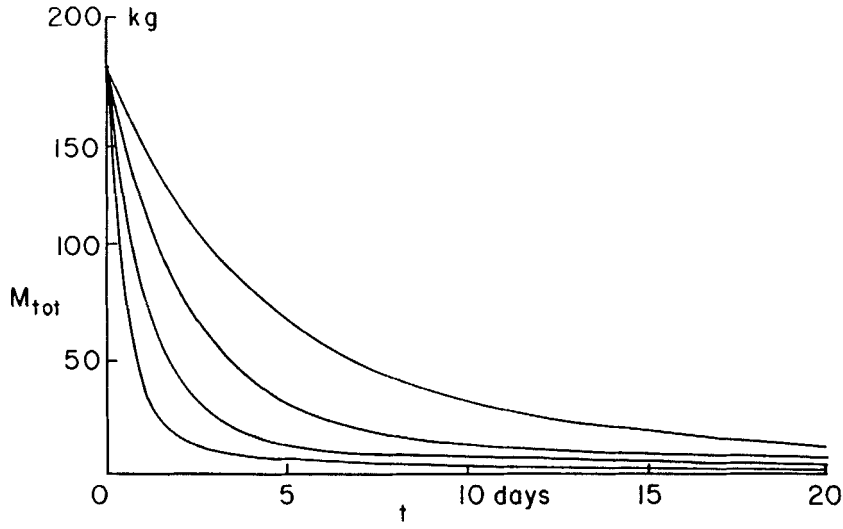

FIG. 12 Plots of total residual VOC mass versus time (no DNAPL present); effect of the sparging air molar flow rate Q_a. In these runs the aqueous-vapor VOC mass transfer rate parameter λ is taken proportional to Q_a. Q_a = 0.125, 0.25, 0.5, and 1.0 mol/s; Q_w = 0.125, 0.25, 0.5, and 1.0 L/s; λ = 0.000125, 0.00025, 0.0005, and 0.001 second^{-1}, top to bottom. Default parameters as in Table 3.

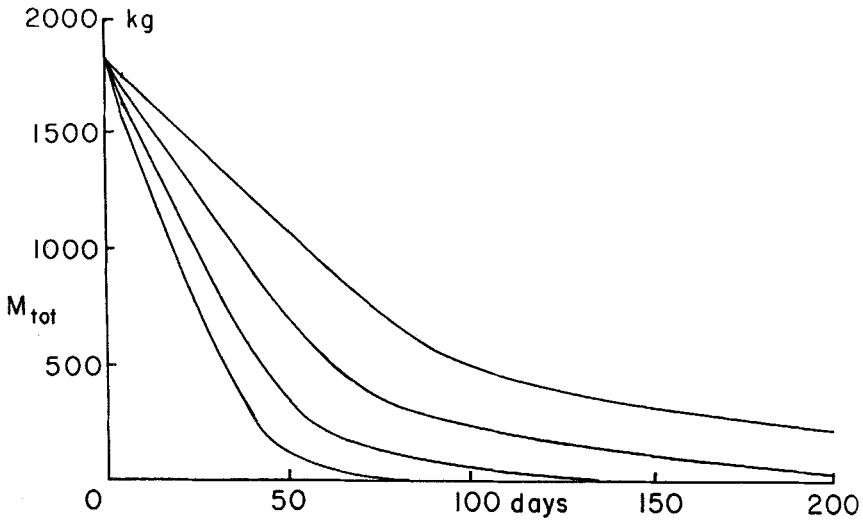

FIG. 13 Plots of residual mass of TCE versus time (DNAPL present); effect of the sparging air molar flow rate Q_a. In these runs the aqueous-vapor VOC mass transfer rate parameter λ is taken proportional to Q_a. Q_a = 0.125, 0.25, 0.5, and 1.0 mol/s; Q_w = 0.125, 0.25, 0.5, and 1.0 L/s; λ = 0.000125, 0.00025, 0.0005, and 0.001 second^{-1}, top to bottom. Default parameters as in Table 2.

the aqueous phase becomes limiting and the curves approach a limiting form.

In conclusion, we note that 1) the model presented requires a rather limited number of input parameters, 2) it runs readily on currently available microcomputers, 3) it permits the modeling of DNAPL solution kinetics and aqueous-vapor mass transport kinetics, and 4) the trends shown by the numerical results appear quite reasonable in the light of physical intuition. It is hoped that the model will prove useful as an evaluation and design tool to people involved with the remediation of aquifers contaminated with VOCs, and that future data from a broad range of sites will provide field validation.

REFERENCES

1. F. Schwille, *Dense Chlorinated Solvents in Porous and Fractured Media: Model Experiments* (J. Pankow, translator), Lewis Publishers, Chelsea, Michigan, 1988.
2. S. Feenstra and J. A. Cherry, "Dense Organic Solvents in Ground Water: An Introduction," in *Dense Chlorinated Solvents in Ground Water*, Institute for Ground Water Research, University of Waterloo, Progress Report 0863985, 1987.

3. S. E. Powers, C. O. Louriero, L. M. Abriola, and W. J. Weber Jr., "Theoretical Study of the Significance of Nonequilibrium Dissolution of Nonaqueous Phase Liquids in Subsurface Systems," *Water Resour. Res.*, *27*, 463 (1991).
4. S. E. Powers, L. M. Abriola, and W. J. Weber Jr., "An Experimental Investigation of Nonaqueous Phase Liquid Dissolution in Saturated Subsurface Systems," *Ibid.*, *28*, 2691 (1992).
5. B. Herrling and J. Stamm, *Vacuum-Vaporizer-Wells for In Situ Remediation of Volatile and Strippable Contaminants in the Unsaturated and Saturated Zone*, Presented at the Symposium on Soil Venting, Houston, Texas, April 29–May 1, 1991, Robert S. Kerr Environmental Research Laboratory and National Center for Ground Water Research, sponsors.
6. R. A. Brown, *Air Sparging—Extending Volatilization to Contaminated Aquifers*, Presented at the Symposium on Soil Venting, Houston, Texas, April 29–May 1, 1991, Robert S. Kerr Environmental Research Laboratory and National Center for Ground Water Research, sponsors.
7. R. A. Brown, *Air Sparging: A Primer for Application and Design*, Groundwater Technology, Inc., 310 Horizon Center Dr., Trenton, New Jersey 08691 (1992).
8. D. J. Wilson, S. Kayano, R. D. Mutch Jr., and A. N. Clarke, "Groundwater Cleanup by *in-situ* Sparging. I. Mathematical Modeling," *Sep. Sci. Technol.*, *27*, 1023 (1992).
9. D. J. Wilson, "Groundwater Cleanup by *in-situ* Sparging. II. Modeling of Dissolved VOC Removal," *Ibid.*, *27*, 1675 (1992).
10. L. A. Roberts and D. J. Wilson, "Groundwater Cleanup by *in-situ* Sparging. III. Modeling of Dense Nonaqueous Phase Liquid Droplet Removal," *Ibid.*, *28*, 1127 (1993).
11. S. D. Burchfield and D. J. Wilson, "Groundwater Cleanup by *in-situ* Sparging. IV. Removal of Dense Nonaqueous Phase Liquid by Sparging Pipes," *Ibid.*, *28*, 2529 (1993).
12. D. J. Wilson, "Soil Clean Up by *in-situ* Aeration. V. Vapor Stripping from Fractured Bedrock," *Ibid.*, *25*, 243 (1990).
13. S. Kayano and D. J. Wilson, "Migration of Pollutants in Groundwater. VI. Flushing of DNAPL Droplets/Ganglia," *Environ. Monitor. Assess.*, *25*, 193 (1993).
14. J. H. Montgomery and L. M. Welkom, *Groundwater Chemicals Desk Reference*, Vols. 1 and 2, Lewis Publishers, Ann Arbor, Michigan, 1990.

Received by editor April 26, 1993